Hue and Saturation Dispersion Modeling. Application to the Improvement of the Segmentation in the HS Sub-space

E. Blanco, M. Mazo, L.M. Bergasa and S. Palazuelos
Department of Electronics
University of Alcalá
Alcalá de Henares, Spain
Email: edward@depeca.uah.es, mazo@depeca.uah.es, bergasa@depeca.uah.es, sira@depeca.uah.es

***Abstract*—In this paper, a modeling of the hue and saturation dispersions of classes projected in the *HS* plane is presented. The relevance of the proposed modeling is its application in general clustering processes in the *HS* domain. In a previous work about class separation in the *HS* plane for segmentation improvement, it was necessary to calculate the hue and saturation variances of the classes for their different locations in the *HS* plane. Classes may be composed by a high number of samples and variances are distinct for the different locations within the *HS* plane, so this process needs a high processing calculus time. In the current paper, the hue and saturation dispersions are modeled (requiring a lower processing time) and are applied to that segmentation process. The authors propose to use the geometric-analytical relationships between the *HSI* space and the YC_1C_2 tristimulus. These relationships allow to estimate the dispersions of the classes projected in the *HS* plane from their dispersions in the C_1C_2 linear chromatic plane. The results obtained in different practical applications show the validity of the proposal and a remarkable improvement in the processing time.**

I. INTRODUCTION

In the image processing area, applications that perform object clustering and segmentation processes are usually based on pixel classification. This pixel classification often uses a distance metric in a sub-space formed by components from one or several color spaces as discriminant function [1-4].

As is known, the calculation or estimation of the class covariance matrixes plays a fundamental role in the classification process operation and performance, because these variances determine the class reliability. Some previous works calculate the mean vectors and the covariance matrix to characterize the classes, (e.g. object and background), in an off-line process, keeping these values constant during the classification process, independently of the kind of classifier used, for example, using a distance metric as the *Mahalanobis* one [3] (in the C_bC_r plane) or Bayesian classifiers [4].

However, in other works, such as "Improvement of the Segmentation in *HS* Sub-space by means of a Linear Transformation in *RGB* Space" [5], previously presented by the authors, the interest and need of the on-line calculation of the object and background class variances in *HS* components are shown. In the proposal presented in [5], an iterative process is executed. This process requires the calculation of the hue and saturation dispersions of the classes in the *HS* plane for each iteration. To avoid the variances calculation in each iteration, the authors propose in the current work a modeling that estimates the hue and saturation deviations in order to reduce the processing time. The proposed model is based on the existing mathematical relationships between the *HSI* color space [6] and the YC_1C_2 space [7-9].

An estimation of the hue and saturation deviation is performed in [10] for the Smith's *HSI* transformation [11]. In [10], the estimation provides a reliability degree of the H and S values which is used to improve the color classification processes.

An analysis of the additive Gaussian noise propagation from *RGB* space to normalized *rg*, to the opponent color space (o_1, o_2) and to a particular hue component (θ) is carried out in [12]. In this last work, approximations of the r, g, o_1, o_2 and θ deviations from the values of R, G and B and their respective deviations are obtained. These approximations are used to obtain several variable kernel density estimations to construct robust histograms.

In the author's previous paper [5], equations to directly convert between *HSI* and YC_1C_2 spaces are demonstrated. Taking C_1C_2 plane as a reference, a geometric-analytical formulation by means of the class uncertainty ellipse in this plane is performed to estimate the hue deviation. Besides, as shown in [5], the saturation component is a linear function of C_1 and C_2 components. Now, we take into account this characteristic to obtain a mathematical expression to estimate the class saturation variance.

This paper has been organized as follows: section II describes the proposed algorithm, starting from an introduction about the existing relationships between the YC_1C_2 and *HSI* spaces, and, afterwards, the proposed modeling of the hue and saturation dispersion. Section III presents the method to apply this modeling to the technique of improvement of the segmentation in the *HS* sub-space by means of a linear transformation described in [5]. Section IV presents the experimental results, and section V the conclusions.

1-4244-0755-9/07/$20.00 ©2007 IEEE

II. PROPOSED METHOD

The processing time needed for the calculation of the hue and saturation variances in each location in the *HS* plane may not fulfill the temporal restrictions required by some real-time application. Therefore, the interest to obtain a mathematical model that requires lower processing time to estimate the hue and saturation variance is justified. This model is particularly important when the class is formed by a high number of samples.

In this section, the modeling of the dispersions of a class in the *HS* plane is presented. This modeling uses the mathematical relationship between the YC_1C_2 and *HSI* spaces.

A. Relationship between YC_1C_2 and HSI spaces

The correspondence between the YC_1C_2 and *HSI* color spaces allows to obtain the modeling of the hue and saturation dispersion, because the linearity property of the YC_1C_2 space can be used to diminish the non-linearity and discontinuity problems of the *HSI* space. In the author's previous work [5] the relationship between both spaces is demonstrated:

$$H=\begin{cases}\alpha, & C_2\geq 0\\ 2\pi-\alpha, & \text{otherwise}\end{cases};\quad \alpha=\cos^{-1}\left(\frac{C_1}{(C_1^2+C_2^2)^{1/2}}\right) \tag{1}$$

$$S=\begin{cases}\dfrac{C_1+\sqrt{3}C_2}{3Y}; & 0<H\leq 2\pi/3\\ -\dfrac{2C_1}{3Y}; & 2\pi/3<H\leq 4\pi/3\\ \dfrac{C_1-\sqrt{3}C_2}{3Y}; & 4\pi/3<H\leq 2\pi\end{cases} \tag{2}$$

$$I=Y \tag{3}$$

In [5], a set of values of a class separation measurement index is obtained applying several translations to the classes in the C_1C_2 plane. As will be shown in the following sections, the class translations are performed by adding a color vector ($\mathbf{i}_r$) to the classes in the *RGB* space, or a translation vector ($\mathbf{i}_c$) to the classes in the C_1C_2 plane. It can be demonstrated that any translation of a class in the C_1C_2 plane always produces a modification of the hue dispersion in the *HS* plane. The hue dispersion value will remain constant if and only if the class geometry in the C_1C_2 plane is circular and the translations are angular, (not radial or a combination of radial and angular). Furthermore, the saturation dispersion is also modified by effect of the variation of the hue dispersion, but a purely angular translation also keeps constant the saturation dispersion, independently of the class geometric form. In general, the geometric form of the classes is not predetermined and the translations applied to a particular class may be both radial and angular.

The objective of this work is to obtain a modeling of the dispersions for any class geometric form and any kind of translation within the *HS* plane.

B. Class Dispersion Modeling

In this section, a modeling to describe the behavior of the hue and saturation dispersions of the classes in the *HS* plane when translated in the C_1C_2 plane is presented. The proposed modeling obtains the value of the hue and saturation deviations as a function of the class means in the C_1C_2 plane (μ_{C1} and μ_{C2}).

1. Modeling of the Hue Dispersion

Given that the angle of a vector $\mathbf{c}$ in the C_1C_2 plane and the angle of a vector $\mathbf{h}$ in the *HS* plane are the same (superposed vectors), the variations of the angular dispersion in the C_1C_2 plane correspond with the variation of the hue dispersion in the *HS* plane [5]. Therefore, if the uncertainty ellipse of the class in the C_1C_2 plane is obtained, the angular deviation can be approximated by half of the angle between the two straight lines tangent to the uncertainty ellipse (one on each side of μ_H) that also pass through the origin of the plane. For a class Ω formed by N samples (k=1,2,..,N), each sample k in the C_1C_2 plane is represented by a vector $\mathbf{c}_k=[C_{1k}\ \ C_{2k}]^T$. Statistically, the set of N samples is characterized by its mean vector $\mathbf{c}=[\mu_{C1}\ \ \mu_{C2}]^T$ and a covariance matrix $\mathbf{\Sigma}$. The parameters of the uncertainty ellipse of the class Ω (the so-called invariants of the dispersion of hue) are obtained from $\mathbf{\Sigma}$ by:

$$\omega=\tan^{-1}\left(C_{2u}/C_{1u}\right),\ u=\sqrt{\lambda_u},\ l=\sqrt{\lambda_l} \tag{4}$$

where ω is the angle of the major axis with respect to the horizontal axis (C_1 axis), u and l are the semimajor and semiminor axes of the ellipse, respectively. C_{1u} and C_{2u} are the components of the eigenvector corresponding to the highest eigenvalue (λ_u) of $\mathbf{\Sigma}$, and λ_l is the lowest one.

A geometric-analytical formulation to relate the standard deviation of the hue (σ_H) of a class in the *HS* plane is performed with the invariants of hue (4) for the different locations of the class in the C_1C_2 plane. Starting from the generic equation of an ellipse in the C_1C_2 plane, it is possible to estimate the σ_H. The ellipse equation as a function of C_1 and C_2, $g(C_1,C_2)$, is given by:

$$aC_1^2+dC_1+bC_1C_2+cC_2+eC_2^2+f=1 \tag{5}$$

where a, b and c are translation invariant coefficients, because they are only a function of (4), and are given by:

$$a=(\cos^2\omega/u^2+\sin^2\omega/l^2),\ b=2\sin\omega\cos\omega(1/u^2-1/l^2),$$
$$c=(\sin^2\omega/u^2+\cos^2\omega/l^2). \tag{6}$$

Here, d, e and f are translation dependent coefficients, because they are a function of the class means: μ_{C1} and μ_{C2}.

$$d=-(2a\mu_{C1}+b\mu_{C2}),\ e=-(2c\mu_{C2}+b\mu_{C1}),$$
$$f=a\mu_{C1}^2+b\mu_{C1}\mu_{C2}+c\mu_{C2}^2. \tag{7}$$

The estimation of σ_H as a function of the parameters μ_{C1} and μ_{C2}, starts by choosing one of the tangency points between the two tangent lines and the ellipse, i.e., $p_t=[C_{1t}\ \ C_{2t}]^T$. Taking the partial derivative of the ellipse equation (5), given by:

$$\frac{\partial g(C_1,C_2)}{\partial C_1}=2aC_1+d+bC_2\,,\ \frac{\partial g(C_1,C_2)}{\partial C_2}=2cC_2+e+bC_1 \quad (8)$$

and knowing that the tangent lines pass through the origin of the coordinates plane, using p_t, the following expression is obtained:

$$\frac{C_{2t}}{C_{1t}}=\frac{2cC_2+e+bC_1}{2aC_1+d+bC_2}\,. \quad (9)$$

The tangency point p_t belongs to the ellipse, therefore, C_{1t} can be obtained from (5) and (9) by:

$$C_{1tj}=\frac{k_a\mathrm{B}\pm\sqrt{k_a(\mathrm{B}^2-4\mathrm{AC})}}{k_b};\ j=\begin{cases}1;\ +\\ 2;\ -\end{cases} \quad (10)$$

where $\mathrm{A}=\mathrm{E}^2-a/c$, $\mathrm{B}=eb/2c^2-d/c$, $\mathrm{C}=\mathrm{E}^2+(1-f)/c$, $k_a=(1-\mathrm{C}/\mathrm{E}^2)$, $k_b=(\mathrm{B}^2/2\mathrm{E}^2-2\mathrm{A})$ and $\mathrm{E}=-e/2c$. Then, using (5) and (10), the C_{2t}'s are obtained by means of:

$$(C_{2t11},C_{2t12},C_{2t21},C_{2t22})=\mathrm{E}+\mathrm{D}C_{1tj}\pm\sqrt{\mathrm{A}C_{1tj}^2+\mathrm{B}C_{1tj}+\mathrm{C}} \quad (11)$$

where $\mathrm{D}=-b/2c$. Four tangency points can be obtained from the last equation (11): $p_{t1}=(C_{1t1},\ C_{2t11})$, $p_{t2}=(C_{1t1},\ C_{2t12})$, $p_{t3}=(C_{1t2},\ C_{2t21})$ and $p_{t4}=(C_{1t2},\ C_{2t22})$. The choice of a particular point depends on the location of the ellipse within the plane, because all of them may be valid. If H_{t1}, H_{t2}, H_{t3} and H_{t4} are the angles produced by these tangency points respectively, the hue deviation is approximated by:

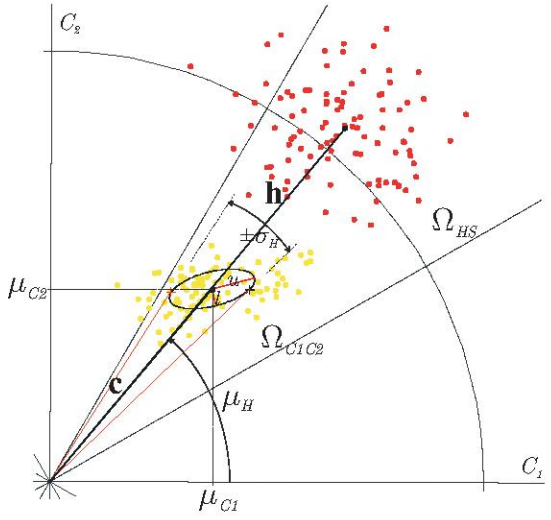

Fig. 1. Correspondence of a class Ω in the C_1C_2 and HS planes. Calculation of the hue deviation by means of the uncertainty ellipse in the C_1C_2 plane.

$$\sigma_H=\frac{1}{2}\left(\max\left(\bar{d}(\mu_H,H_{tn})\right)-\min\left(\bar{d}(\mu_H,H_{tn})\right)\right);n=1,2,3,4 \quad (12)$$

where $\bar{d}(\mu_H,H_{tn})$ is the known *directed distance*, created to avoid the problems of the cyclic property of the Hue seen in [9]. Here, the *directed distance* between the angle of each tangency point and the angular mean is obtained.

Fig. 1 depicts the correspondence of a class in both domains, HS and C_1C_2. The mean vector **c** of the class in the C_1C_2 plane (Ω_{C1C2}) and its corresponding mean vector **h** of the class in the HS plane (Ω_{HS}) are shown. The calculation of the angular or hue deviation (σ_H), by means of the uncertainty ellipse of the class in the C_1C_2 plane can also be observed.

2. *Modeling of the Saturation Dispersion*

The dispersion of the saturation component is not directly affected by the translations of the classes in the C_1C_2 plane, but for the variation of the class samples intensities (Y). The reason is that saturation is a linear function of the C_1 and C_2 components and varies inversely with Y, as (2) shows. In this sense, it can be demonstrated that the saturation deviation (σ_S) remains constant if all the intensity values of the class are equal. In this paper, an equation to model the behavior of the σ_S of a class when it moves in the HS plane, as a function of its mean in the C_1C_2 plane (μ_{C1} and μ_{C2}), has been obtained.

The first step to model the saturation dispersion is to choose one of the tree color sectors delimited by the tree discontinuities of the saturation function (2). For the (0-2π/3) sector, from the definition of variance and using (2), the following expression is obtained:

$$\sigma_S^2=\frac{1}{N}\sum_{k=1}^{N}\left((C_{1k}+\sqrt{3}C_{2k})/3Y_k-(\mu_{C1}+\sqrt{3}\mu_{C2})/\mu_Y\right)^2. \quad (13)$$

Knowing that the C_{1k} and C_{2k} components can be expressed as a function of the class mean, i.e., $C_{1k}=(\mu_{C1}+\Delta_k)$ and $C_{2k}=(\mu_{C2}+\nabla_k)$, where Δ_k and ∇_k are the increments in C_{1k} and C_{2k} with respect to its mean, and substituting in (13), the saturation variance as a function of the class mean is obtained:

$$\sigma_S^2=k_N(a_s\mu_{C1}^2+d_s\mu_{C1}+b_s\mu_{C1}\mu_{C2}+e_s\mu_{C2}+c_s\mu_{C2}^2+f_s) \quad (14)$$

where,

$$\begin{aligned}&k_N=1/(9N),a_s=(k_1-2k_7/\mu_Y),b_s=2\sqrt{3}a_s,c_s=3a_s,\\ &d_s=2(k_2+\sqrt{3}k_4-k_8/\mu_Y-\sqrt{3}k_9/\mu_Y),\\ &e_s=2(\sqrt{3}k_2+3k_4-\sqrt{3}k_8/\mu_Y-3k_9/\mu_Y),f_s=(k_3+2\sqrt{3}k_5+3k_6).\end{aligned} \quad (15)$$

In (15) $k_1=\mathbf{u}^T(\mathbf{Y}^2)^{-1}\mathbf{u}$, $k_2=\mathbf{u}^T(\mathbf{Y}^2)^{-1}\boldsymbol{\Delta}$, $k_3=\boldsymbol{\Delta}^T(\mathbf{Y}^2)^{-1}\boldsymbol{\Delta}$, $k_4=\mathbf{u}^T(\mathbf{Y}^2)^{-1}\boldsymbol{\nabla}$, $k_5=\boldsymbol{\Delta}^T(\mathbf{Y}^2)^{-1}\boldsymbol{\nabla}$, $k_6=\boldsymbol{\nabla}^T(\mathbf{Y}^2)^{-1}\boldsymbol{\nabla}$, $k_7=\mathbf{u}^T\mathbf{Y}^{-1}\mathbf{u}$, $k_8=\mathbf{u}^T\mathbf{Y}^{-1}\boldsymbol{\Delta}$ and $k_9=\mathbf{u}^T\mathbf{Y}^{-1}\boldsymbol{\nabla}$; where **u** is a Nx1 auxiliary vector formed by 1's. **Δ**, **∇** and **Y** are expressed by:

$$\boldsymbol{\Delta}=[\Delta_1\Delta_2...\Delta_N]^T,\ \boldsymbol{\nabla}=[\nabla_1\nabla_2...\nabla_N]^T,\ \mathbf{Y}=\begin{bmatrix} Y_1 & 0 & \cdots & 0 \\ 0 & Y_2 & \cdots & 0 \\ \vdots & \vdots & \ddots & \vdots \\ 0 & 0 & \cdots & Y_N \end{bmatrix}. \quad (16)$$

$\boldsymbol{\Delta}$, $\boldsymbol{\nabla}$ and $\mathbf{Y}$ remain constant in the translation and are called invariants of the dispersion of saturation. As can be seen, $\boldsymbol{\Delta}$ and $\boldsymbol{\nabla}$ indirectly represent the mean deviations of the components of the class in the C_1C_2 plane, and μ_Y=E{diag($\mathbf{Y}$)}.

In the range ($2\pi/3$–$4\pi/3$) the coefficients are:

$$\begin{aligned} &k_N=4k_N,\ a_s=(k_1-2k_7/\mu_Y),\ b_s=0,\ c_s=0, \\ &d_s=2(k_2-k_8/\mu_Y),\ e_s=0,\ f_s=k_3. \end{aligned} \quad (17)$$

Substituting the values of (17) in (14), a quadratic equation in the variable μ_{C1} is obtained. This is due to the saturation expression in this range that depends only on the C_1 component (2).

In the range ($4\pi/3$–2π) the coefficients are given by:

$$\begin{aligned} &k_N=1/(9N),\ a_s=(k_1-2k_7/\mu_Y),\ b_s=-2\sqrt{3}a_s,\ c_s=3a_s, \\ &d_s=2(k_2-\sqrt{3}k_4-k_8/\mu_Y+\sqrt{3}k_9/\mu_Y), \\ &e_s=2(-\sqrt{3}k_2+3k_4+\sqrt{3}k_8/\mu_Y-3k_9/\mu_Y),\ f_s=(k_3-2\sqrt{3}k_5+3k_6). \end{aligned} \quad (18)$$

III. Application of the Proposed Modeling to the Preexistent Technique to Improve the Segmentation in the *HS* Sub-space

The technique to improve the segmentation in the HS sub-space by means of a linear transformation in the RGB space has been recently published in [5]. The linear transformation described in [5] consists on adding a vector in RGB components (in principle, a zero-mean vector) to each captured RGB image, to obtain a higher separation between the object and background classes in the HS plane. As a result, the segmentation of the desired object in the HS plane is improved. This technique takes advantage of the non-linearities produced by the HSI space to achieve a higher separation between the classes. The goal of the algorithm proposed in [5] is to obtain an optimal vector ($\mathbf{i}_r$) to add. This vector has a direct relationship with the separation angle (θ_{in}) between the mean vectors of the classes in the C_1C_2 plane ($\mathbf{c}_{iO}$ and $\mathbf{c}_{iB}$) and, therefore, of the mean vectors $\mathbf{h}_{iO}$ and $\mathbf{h}_{iB}$ of the same classes in the HS plane. The algorithm proposed in [5] has been parameterized as a function of the separation angle (θ_{in}). In the first phases of the algorithm, the classes in RGB are transformed to the YC_1C_2 space, the mean vectors of both classes are calculated ($\mathbf{c}_O$ and $\mathbf{c}_B$), and the difference vector $\mathbf{d}_c$ between them is obtained. The invariants are obtained from $\mathbf{d}_c$ (magnitude $\|\mathbf{d}_c\|$ and phase ϕ of $\mathbf{d}_c$). Afterwards, an iterative process to obtain the optimal $\mathbf{i}_r$ is executed. In each iteration: the value of θ_{in} is increased by $\Delta\theta$, the translation vector $\mathbf{i}_c$ corresponding to that increment is obtained, both classes are translated in the C_1C_2 plane and transformed to the HS plane, and afterwards, the class separation measurement index β_{HSn} is obtained. Finally, this value β_{HSn} is registered. This process is repeated until a θ_{in} that produces the RGB values of the mean vectors higher than one is obtained. This β_{HSn} is a normalized measurement index obtained from the particularized Fisher Ratio (FR), defined as:

$$FR_H=\theta_{in}/\sqrt{\sigma_{HO}^2+\sigma_{HB}^2},\ FR_S=\|d_S\|/\sqrt{\sigma_{SO}^2+\sigma_{SB}^2} \quad (19)$$

where FR_H and FR_S are the FR of the H and S components respectively; d_S=μ_{SO}−μ_{SB} is the distance between the saturation means of both classes, σ_{SO} and σ_{SB} are the standard deviations of the saturation for both classes and, finally, σ_{HO} and σ_{HB} are the hue deviations. The measurement index is given by:

$$\beta_{HSn}=k_h\beta_{Hn}+(1-k_n)\beta_{Sn} \quad (20)$$

where β_{Hn}=(FR_H−1)/FR_H, β_{Sn}=(FR_S−1)/FR_S and k_h is a weighting factor that takes values between 0 and 1.

The proposal described in section II is used for each class to obtain the deviations (σ_{SO}, σ_{SB}, σ_{HO} and σ_{HB}) implied in the calculation of β_{Hn} and β_{Sn} (19). In this sense, the main contribution of this work is using only the expressions dependent on the translations to estimate the deviations in the iterative process to obtain the optimal vector $\mathbf{i}_r$ to add. That is, (7), (10-12) are used for the estimation of the hue deviation (σ_H) and (14) is used for the saturation deviation (σ_S). The use of (14) is conditioned by the range where the class is located, using the coefficients given in (15), (17) or (18). It is important to note that those coefficients are not recalculated in each iteration, implying a remarkable reduction in the processing time. After the iterative process, the algorithm ends with the calculation of the maximum of the observation function formed by the pairs (β_{HSn}, θ_{in}), obtaining an optimal θ_{in} (θ_{opt}) when β_{HSn} is maximum. The vector to add $\mathbf{i}_r$ is obtained with this θ_{opt}.

IV. Experimental Results

The effectiveness of the proposed method has been evaluated using a bank of real images. The technique of segmentation improvement of [5] adding the modeling proposed in this paper has been applied. Fig. 2 and Fig. 3 present two illustrative examples that show the hue and saturation deviation curves, calculated (measured) and estimated by means of the proposed modeling. The curves for both classes, object (O) and background (B), are shown. Fig. 4 depicts the curves of the class separation measurement indexes β_{HSn}, real and approximated, obtained from the calculated and estimated deviations for both cases. All these curves are displayed as a function of the angle $\theta_{in}/2$. In the first stage of the tests N=50 samples were used and the increment of the iterative process was $\Delta\theta$=5.

Table I shows the errors produced when estimating the hue

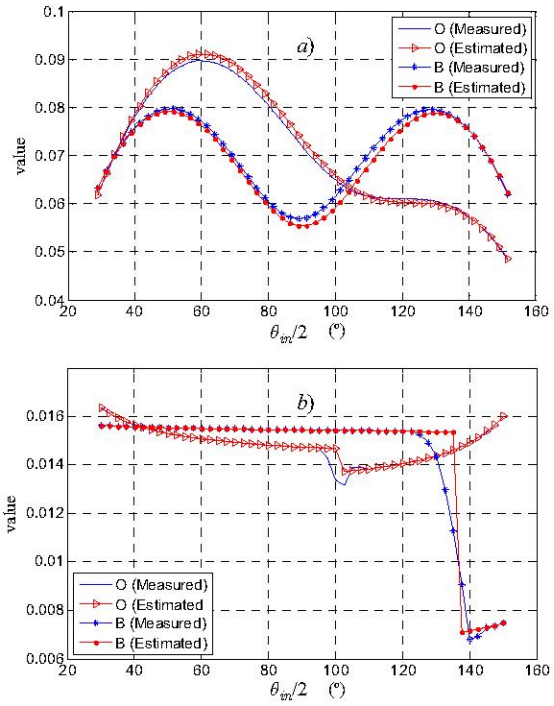

Fig. 2. Curves of calculated (measured) and estimated deviations for case 1: *a*) hue deviations for both classes, *b*) saturation deviations.

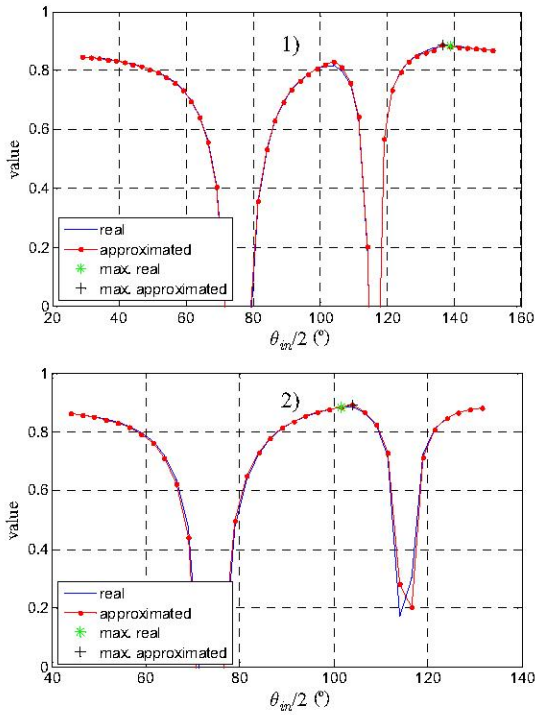

Fig. 4. Class separation measurement indexes (β_{HSn}), real and approximated, for both cases: 1) case1 and 2) case 2.

and saturation deviations for five cases of the image bank. The estimation errors (Error) in RMS (Root Mean Squared) values and the error percentages (%E) can be observed. The values Error and %E are obtained for both classes (O and B).

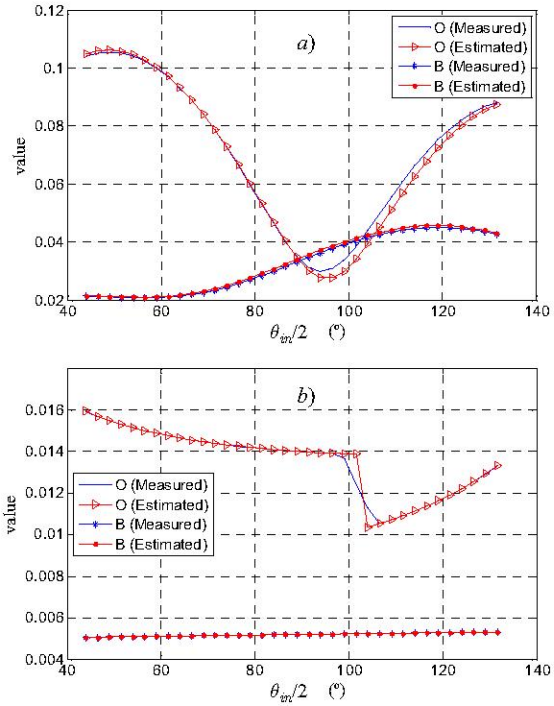

Fig. 3. Curves of calculated (measured) and estimated deviations for case 2: *a*) hue deviations for both classes, *b*) saturation deviations.

In order to evaluate the efficiency of the proposed modeling in processing time, diverse tests have been carried out using the iterative algorithm of the segmentation improvement technique proposed in [5]. Different number of samples (N=50, 100, 200, 500) has been used in these tests, in a PC with Intel Centrino processor at 1.5GHz. In Table II, the processing times (average) required by the iterative process for the 5 cases of Table I along with the number of iterations (m) are presented. The processing time obtained calculating the variances in each iteration is identified by CPT (variance Calculation Processing Time), and the processing time if the variances are estimated (proposal of this paper) is identified by EPT (variance Estimation Processing Time).

TABLE I
ERRORS OF THE ESTIMATION FOR FIVE EXAMPLES

case	Hue deviation				Saturation deviation			
	O class		B class		O class		B class	
	Error (RMS)	%E	Error (RMS)	%E	Error (RMS)	%E	Error (RMS)	%E
1	$1.48\text{x}10^{-3}$	2.04	$2.24\text{x}10^{-3}$	2.88	$0.24\text{x}10^{-3}$	1.98	$0.88\text{x}10^{-3}$	5.56
2	$6.94\text{x}10^{-3}$	7.49	$0.46\text{x}10^{-3}$	1.72	$0.33\text{x}10^{-3}$	2.05	$0.88\text{x}10^{-8}$	$2.3\text{x}10^{-3}$
3	$22.51\text{x}10^{-3}$	15.38	$1.61\text{x}10^{-3}$	2.12	$4.60\ \text{x}10^{-3}$	10.93	$0.79\ \text{x}10^{-3}$	7.93
4	$5.42\text{x}10^{-3}$	6.51	$1.39\ \text{x}10^{-3}$	3.06	$1.06\ \text{x}10^{-3}$	6.77	$0.30\ \text{x}10^{-3}$	4.53
5	$4.57\text{x}10^{-3}$	7.39	$1.52\ \text{x}10^{-3}$	3.75	$0.36\ \text{x}10^{-3}$	2.62	$0.62\ \text{x}10^{-3}$	9,47

Table II shows that processing times when the proposed modeling is applied (EPT) are lower than the processing times if it is not applied (CPT). This conclusion is valid for all the N values. Independently of N, it could be said that EPT is practically constant, as depicted in Fig. 5. That figure shows

how CPT considerably increases as N increases, while EPT remains constant. This method guarantees real-time processing even with very high N values, a big problem in some segmentation applications.

TABLE II
FIVE EXAMPLES CPU TIMES

case	m	CPU Times (milliseconds)							
		N=50		N=100		N=200		N=500	
		CPT	EPT	CPT	EPT	CPT	EPT	CPT	EPT
1	49	59.1	19.0	92.2	18.9	180.1	18.9	519.9	19.1
2	37	46.5	15.2	70.9	14.9	131.4	14.8	415.7	15.3
3	59	73.9	21.6	115.6	21.2	215.6	21.3	653.4	21.3
4	46	58.1	17.8	91.4	17.8	170.9	17.6	607.7	17.9
5	51	62.8	19.2	100.9	19.4	190.7	19.5	576.5	19.2

Finally, after applying the segmentation improvement technique of [5] and adding the modeling proposed in this paper, two experimental tests of segmentation for the image bank have been performed. Fig. 6 shows the results of these segmentations, where the left image is the original one, the central image has been segmented with the technique of [5] and in the right image, the technique of [5] along with the proposed modeling of the hue and saturation dispersions has been applied. It can be observed that the technique including the estimation of the variances by means of the proposed modeling produces similar results in the skin color segmentation.

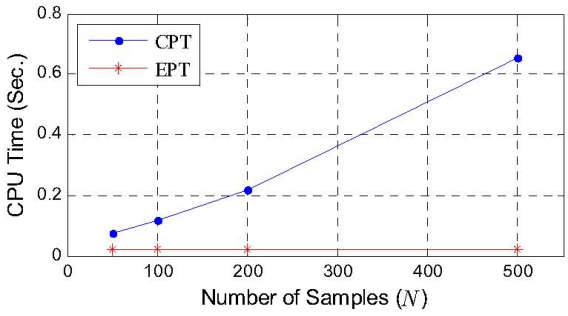

Fig. 5. Curves of processing times: calculating the variances (CPT) and estimating the variances by means of the proposed modeling (EPT).

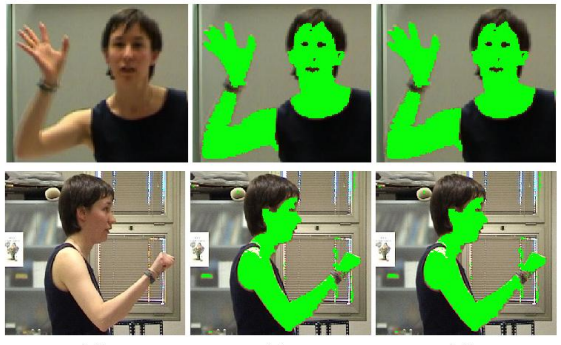

Fig. 6. Results of the segmentations: (a) original images, (b) images segmented with the technique of [5], (c) images segmented with the technique of [5] along with the proposed modeling.

V. CONCLUSIONS

A method to model the dispersion of the classes projected in the *HS* plane as a function of the respective class mean in the C_1C_2 linear chromatic plane has been presented.

It has been demonstrated that the proposed modeling of the hue and saturation dispersions has a good accuracy and very low processing time independently of N samples. Therefore, it can be used in different segmentation alternatives in real-time applications, such as the one proposed in [5] (where the hue and saturation variances were calculated instead of modeled).

When the modeling is applied, the results show a segmentation quality similar to the obtained in [5], with the advantage of a remarkable reduction in the processing time.

ACKNOWLEDGMENT

The work described in this paper has been supported by Ministry of Education and Science (MEC) through the project RESELAI (REF-TIN2006-14896-C02-01).

REFERENCES

[1] N. Vandenbroucke, L. Macaire and J.-G. Postaire, "Color Image Segmentation by Supervised Pixel Classification in a Color Texture Feature Space. Application to soccer image segmentation", *Proc. IEEE 15th Int'l Conf. Pattern Recognition*, Vol. 3, pp. 621–624, 3–7 Sept. 2000.

[2] N. Kehtarnavaz, J. Monaco, J. Nimtschek and A. Weeks, "Color Image Segmentation Using Multi-scale Clustering", *Proc. IEEE Southwest Symp. Image Analysis and Interpretation*, pp. 142–147, 5–7 April 1998.

[3] N. Habili, C. C. Lim and A. Moini, "Segmentation of the Face and Hands in Sign Language Video Sequences Using Color and Motion cues", *IEEE Trans. Circuits and Systems for Video Technology*, Vol. 14, Issue: 8, pp. 1086–1097, Aug. 2004.

[4] S.L. Phung, A. Bouzerdoum and D. Chai, "Skin Segmentation Using Color Pixel Classification: Analysis and Comparison", *IEEE Trans. Pattern Analysis and Machine Intelligence*, Vol. 27, Issue 1, pp. 148–154, Jan 2005.

[5] E. Blanco, M. Mazo, L.M Bergasa, S. Palazuelos and A.B. Awawdeh, "Improvement of the Segmentation in HS Sub-space by means of a Linear Transformation in RGB Space", *Proc. IEEE International Joint Conferences on Computer, Information, and Systems Sciences, and Engineering CISSE06*, 4–14 Dec. 2006.

[6] R.C. Gonzalez and R. E. Woods, "Digital Image Processing", Second Edition, Prentice-Hall Inc., New Jersey, pp. 299, 2002.

[7] T. Carron and P. Lambert, "Color Edge Detector Using Jointly Hue, Saturation and Intensity", *Proc. IEEE Int'l Conf. Image Processing*, Vol. 3, pp. 977–981, 13–16 Nov. 1994.

[8] T. Carron and P. Lambert, "Symbolic Fusion of Hue-Chroma-Intensity Features for Region Segmentation", *Proc. IEEE Int'l Conf. Image Processing*, Vol. 1, pp. 971–974, 16–19 Sept. 1996.

[9] C. Zhang and P. Wang, "A New Method of Color Image Segmentation Based on Intensity and Hue Clustering", *Proc. IEEE 15th Int'l Conf. Pattern Recognition*, Vol. 3, pp. 613–616, 3–7 Sept. 2000.

[10] S. Romaní, P. Sobrerilla and E. Montseny, "On the Reliability Degree of Hue and Saturation Values of a Pixel for Color Image Classification", *The 14th IEEE International Conference on Fuzzy Systems* FUZZ '05, pp. 306–311, May 22-25, 2005.

[11] A.R. Smith, "Color Gamut Transform Pairs," Computer Graphics 12, pp. 12–19, 1978.

[12] T. Gevers and H. Stokman, "Robust Histogram Construction from Color Invariants for Object Recognition", *IEEE Trans. Pattern Analysis and Machine Intelligence*, Vol. 26, Issue 1, pp.113–118, Jan. 2004.